Macromolecules
ARTICLE

Macromolecules **2010**, *43*, 2873–2879 **2873**
DOI: 10.1021/ma100039q

Synthesis of Thieno[3,4-*b*]pyrazine-Based and 2,1,3-Benzothiadiazole-Based Donor−Acceptor Copolymers and their Application in Photovoltaic Devices

Erjun Zhou,[†] Junzi Cong,[†] Shimpei Yamakawa,[‡] Qingshuo Wei,[‡] Motoshi Nakamura,[‡] Keisuke Tajima,[‡] Chunhe Yang,[†] and Kazuhito Hashimoto*,[†,‡]

[†]*HASHIMOTO Light Energy Conversion Project, ERATO, Japan Science and Technology Agency (JST), and* [‡]*Department of Applied Chemistry, School of Engineering, The University of Tokyo, 7-3-1 Hongo, Bunkyo-ku, Tokyo 113-8656, Japan*

Received January 7, 2010; Revised Manuscript Received February 10, 2010

ABSTRACT: Two kinds of thieno[3,4-*b*]pyrazine-based monomers, 2,3-dimethyl-5,7-di(2-bromothien-5-yl)-thieno[3,4-*b*]pyrazine and 2,3-diphenyl-5,7-di(2-bromothien-5-yl)-thieno[3,4-*b*]pyrazine, were synthesized via an improved synthetic route. These two monomers and 4,7-di(2-bromothien-5-yl)-2,1,3-benzothiadiazole were copolymerized with three donor segments (fluorene, carbazole, and indolocarbazole) separately by a Suzuki cross-coupling reaction to give six types of 5,7-dithien-2-yl-thieno[3,4-*b*]pyrazine (DTTP)-based donor−acceptor (D−A) copolymers (TP1-6) and three types of 5,7-dithien-2-yl-2,1,3-benzothiadiazole (DTBT)-based D−A copolymers (PF-DTBT, PC-DTBT, and PIC-DTBT). The optical properties, electrochemical behavior, and energy levels of these nine copolymers were investigated. The photovoltaic performance of the copolymers was compared and discussed considering their energy levels.

Introduction

In the past decade, polymer solar cells (PSCs) have received a great deal of attention as a potential renewable energy source because of their advantages such as low cost, light weight, and capability of fabricating flexible large-area devices.[1] To achieve high performance in optoelectronic devices, it is critical to tune physical properties such as solubility, band gap, molecular energy level, and carrier mobility by chemically modifying the polymer structure.

For photovoltaic polymers, the most widely investigated one is regioregular poly(3-hexylthiophene) (P3HT). Power conversion efficiency (PCE) of 4 to 5% has been achieved in PSCs using the blend of P3HT and [6,6]-phenyl-C_{61}-butyric acid methyl ester (PCBM) by thermal annealing after device fabrication to construct the nanomorphology of the interpenetrating network.[2] However, P3HT has a relatively large band gap (~2.0 eV) and only harvests photons with wavelength below 650 nm, which is a small portion of the whole solar spectrum. Therefore, the design and preparation of novel photovoltaic polymers with broader absorption of solar light, especially in the longer wavelength region, are important challenges to be addressed at present.[3] Many works have demonstrated that alternating electron-rich (donor) and electron-deficient (acceptor) units in the polymer chain is an effective strategy for tuning the properties of polymers, especially to reduce the band gap.[4] By using this strategy, many novel low band gap polymers have been synthesized and used in PSCs with PCEs over 7% combined with intensive device engineering efforts.[5]

Among the large variety of acceptor segments, 4,7-dithien-2-yl-2,1,3-benzothiadiazole (DTBT), linking two thiophene rings in the 4,7-position of 2,1,3-benzothiadiazole (BT), has been developed and copolymerized with many types of donor segments, such as pyrrole,[6] didecyloxyphenylene,[7] fluorene,[8] carbazole,[9] silafluorene (or dibenzosilole),[10] indeno[2,1-*a*]indene,[11] cyclopenta-[2,1-*b*:3,4-*b*]dithiophene,[12] dithienosilole,[13] dithieno[3,2-*b*:2′,3′-*d*]-pyrrole,[14] and indolo[3,2-*b*]carbazole.[15] When these materials have been applied to PSCs, PCEs in the range of 0.41 to 6.1% have been achieved. 5,7-Dithien-2-yl-thieno[3,4-*b*]pyrazine (DTTP) is an isomer of DTBT and has also been studied for designing photovoltaic polymers.[16] However, a detailed comparison of the two isomers in the D−A copolymers has not been done, and the effects of different substituted groups at the 2,3-position of thieno[3,4-*b*]pyrazine (TP) segment remains unclear.

In this article, we report an improved route for the synthesis of two types of 2,3-disubstituted DTTPs: 2,3-dimethyl-5,7-di(2-bromothien-5-yl)-thieno[3,4-*b*]pyrazine and 2,3-diphenyl-5,7-di(2-bromothien-5-yl)-thieno[3,4-*b*]pyrazine. We also report the copolymerization of these two acceptor segments with three well-known donor segments: fluorene, carbazole, and indolo[3,2-*b*]carbazole. Furthermore, the preparation of copolymers combining DTBT and these three donor segments was also conducted for comparison. The optical, electrochemical, and photovoltaic properties of these nine D−A copolymers are compared in detail.

Results and Discussion

Material Synthesis. The reported synthetic route to monomers **5a**[16a] and **5b**[16b] (Scheme 1) is as follows: reduction of 3′,4′-dinitro-2,2′:5′2″-terthiophene (**2**) with $SnCl_2$ to produce 3′,4′-diamino-2,2′:5′2″-terthiophene (**3**) and condensation of **3** with 1,2-diketones to yield 2,3-disubsititued-5,7-di(2-thienyl)-thieno[3,4-*b*]pyrazine, which is brominated with *N*-bromosuccinimide (NBS) to afford the target compound **5**. The difficulty with this route is in the last step, where mono-, di-, and tribrominated products are formed, which are difficult to separate because of their poor solubility and similar R_f values. Furthermore, if one wants to obtain monomer **5** containing different substituted groups such as **5a** and **5b**, one must repeat the bromination step and the time-consuming separation of the brominated products.

*Corresponding author. E-mail: hashimoto@light.t.u-tokyo.ac.jp.

Published on Web 02/22/2010

Scheme 1. Reported Synthetic Routes to 4,7-Di(2-bromothien-5-yl)-2,1,3-benzothiadiazole[17] and 2,3-Disubstituted-5,7-di(2-bromothien-5-yl)-thieno[3,4-*b*]pyrazine[16a,b]

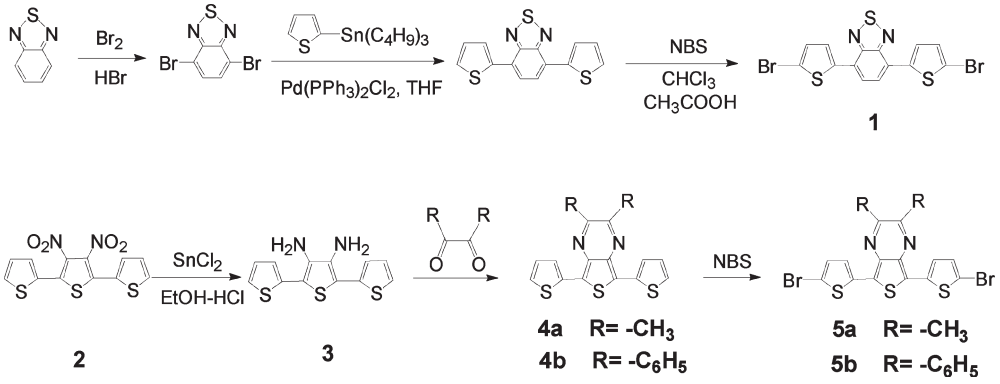

Scheme 2. Improved Synthetic Routes to 2,3-Disubstituted-5,7-di(2-bromothien-5-yl)-thieno[3,4-*b*]pyrazine

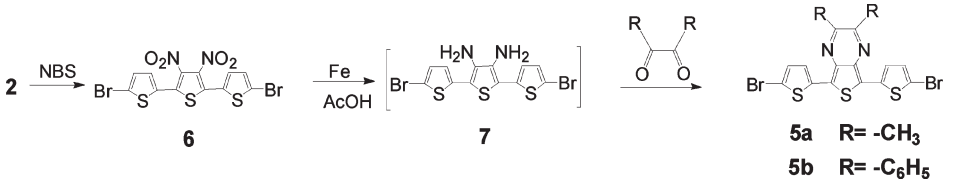

Here an improved synthetic route (Scheme 2) was developed. First, 3′,4′-dinitro-2,2′:5′2″-terthiophene was brominated with NBS in DMF to afford only the dibrominated product **6**. Reduction of **6** with iron in acetic acid produced the diamine **7**, which was found to react with 1,2-diketones very effectively without purification to afford the target compounds **5a** and **5b**. This proposed synthetic route provides more facile access to the target compounds than the previous one. The yield from **6** to monomer **5** was acceptable (~70%), and the purification was much simpler. The total yield from **2** to **5a** was also improved from ~22% by the previous route[16b] to ~60% by the present route.

Nine D−A copolymers were synthesized from the combination of three donor units (**8**, **9**, and **10**) with three acceptor units (**1**, **5a**, and **5b**) by the Suzuki cross-coupling reaction (Scheme 3). To avoid the formation of a large insoluble fraction of polymers, we used a feed molar ratio of donor to acceptor segments that was 100:95. The yield, number-average molecular weight (M_n), weight-average molecular weight (M_w), and polydispersity indices (PDIs) are summarized in Table 1. Most polymerization reactions yielded over 50% after purification by Soxhlet extraction. (See the Experimental Section.) The reactions involving the carbazole showed slightly lower yield; this result could be attributed to the poor solubility of the resulting polymers, the alkyl chain of which does not provide sufficient flexibility to compensate for the rigidity of the acceptor units.

All polymers exhibited excellent thermal stability with onset decomposition temperatures around 300−387 °C in air measured shown by thermogravimetric analysis (TGA). The data are summarized in Table 1. The high thermal stability of these polymers is adequate for application in PSCs or other optoelectronic devices.

Optical Properties. The UV−vis absorption spectra of the nine copolymers in $CHCl_3$ solutions are shown in Figure 1. All polymers exhibited two major absorption bands in the ranges of 300−500 and 500−800 nm. The peak at longer wavelength could be attributed to the intramolecular charge-transfer (ICT) transition, and the other at shorter wavelength was the result of a higher energy transition. The 2,3-diphenyl-DTTP-based polymers showed higher relative absorption in the shorter wavelength range, which might be due to an electronic transition related to the peripheral phenyl rings. Compared with the DTBT-based polymers (PF-DTBT, PC-DTBT, and PIC-DTBT), the 2,3-dimethyl-DTTP-based polymers (TP1, TP3, and TP5) and the 2,3-diphenyl-DTTP-based polymers (TP2, TP4, and TP6) had broader absorption ranges. TP1, TP3, and TP5 had absorption maxima in the longer wavelength range at 577−590 nm with absorption coefficients that were ~20% less, and TP2, TP4, and TP6 had the maxima at 635−651 nm with absorption coefficients that were ~40% less, which were red-shifted by about 50 and 100 nm relative to the DTBT-based polymers, respectively. The shape and the position of the absorption peaks and the absorption coefficients seemed to be determined mainly by the identity of the acceptor segment, and the effects of the donor segment were small. Because of the differences in the absorption spectra, the copolymers showed quite different colors in solution: red for DTBT-based polymers (PF-DTBT, PF-DTBT, and PF-DTBT), blue for 2,3-dimethyl-DTTP-based polymers (TP1, TP3, and TP5), and green for 2,3-diphenyl-DTTP-based polymers (TP2, TP4, and TP6).

The absorption spectra of the nine polymers in thin films are shown in Figure 2, and the optical properties are summarized in Table 2. The shape of the peaks and the trend of the absorption wavelength were generally similar to those in solution. The absorption maxima in the films were red-shifted by 2−23 nm compared with those in solution, suggesting that intermolecular interactions were present in the solid state but were probably not as strong as those for regioregular P3HT.

Electrochemical Properties. The electrochemical properties of the nine polymers were investigated by cyclic voltammetry (CV). The CV curves were recorded referenced to a Ag/Ag^+ (0.01 M of $AgNO_3$ in acetonitrile) electrode, which was calibrated against the ferrocene−ferrocenium (Fc/Fc^+) redox couple (4.8 eV below the vacuum level). The cyclic voltammetric curves are shown in Figure 3. The 2,3-diphenyl-DTTP-based polymers (TP2, TP4, and TP6) showed reversible reduction, whereas others exhibited irreversible reduction at lower potentials. This indicates that the

Scheme 3. Synthetic Routes to Three DTBT-Based D−A Copolymers and Six DTTP-Based D−A Copolymers

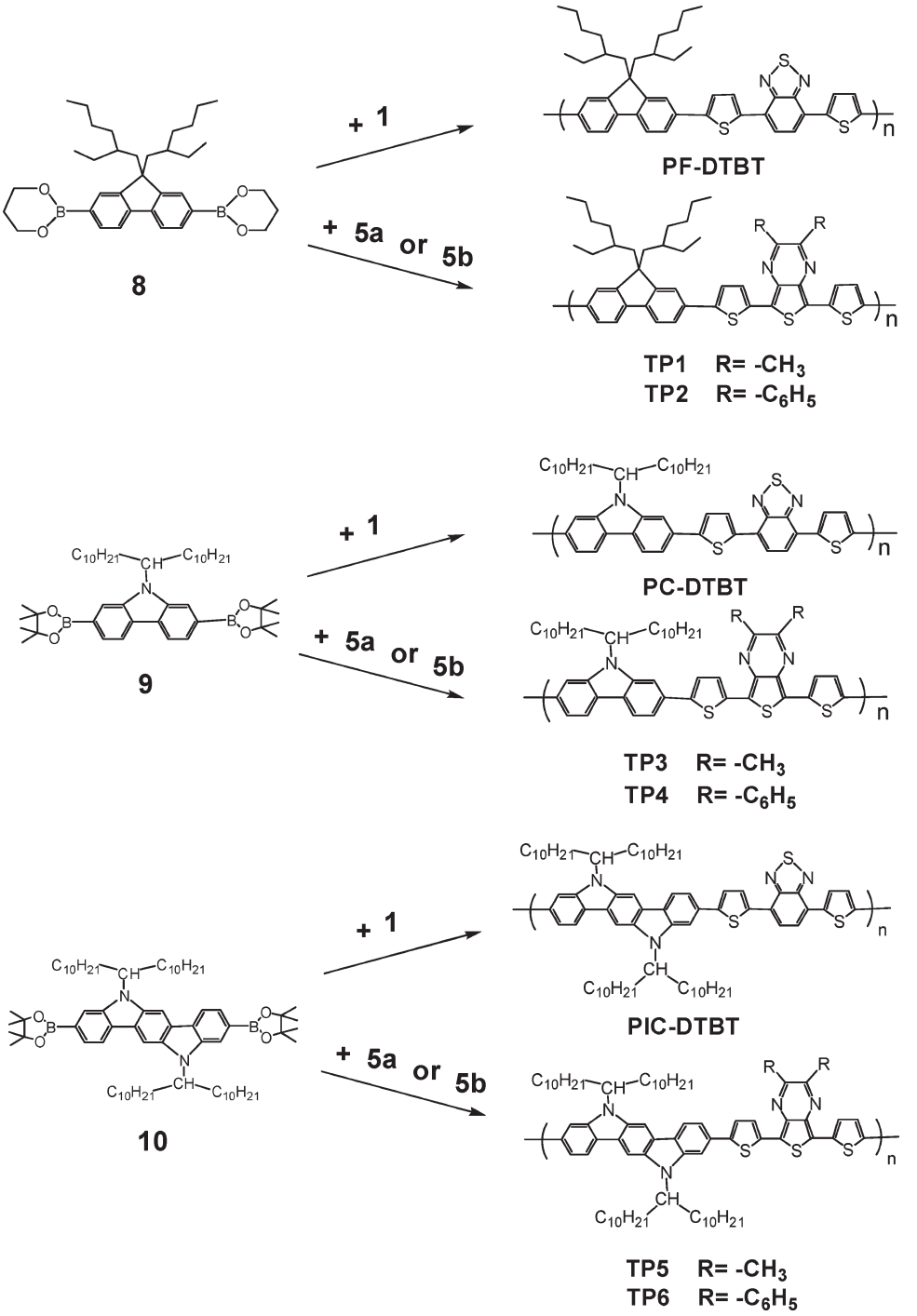

2,3-diphenyl-DTTP-based polymers can accept electron easier than the others and are stable in the reduced state. Considering the differences between the 2,3-diphenyl-DTTP and 2,3-dimethyl-DTTP, the existence of phenyl rings at the 2,3-positions is probably responsible for the higher stability of the reduced state compared with the methyl derivatives. All polymers exhibited quasi-reversible behavior in electrochemical oxidation. The onset potential of DTTP-containing polymers was lower than that of DTBT-contained polymers. The HOMO and the LUMO energy levels of the conjugated polymers were calculated from the value of the onset oxidation potential (E_{on}^{ox}) and the onset reduction potential (E_{on}^{red}); the HOMO and the LUMO are listed in Table 2. Compared with the three corresponding DTBT-based polymers (PF-DTBT, PC-DTBT, and PIC-DTBT), the six DTTP-based polymers (TP1-6) had similar LUMO energy levels, but the HOMO energy levels shifted upward by 0.13 to 0.3 eV, which reduce the band gap of the DTTP-based polymers. This might be due to better delocalization of electrons in the HOMO of the DTTP-based polymers because the three thiophene rings in the DTTP unit impart the molecule with better planarity compared with the one benzene and two thiophene rings in DTBT. For all nine polymers, the electrochemical band gap (E_g^{EC}) was slightly larger than the optical band gap (E_g^{opt}), which was calculated from the onset of the absorption spectra in the films.

Photovoltaic Properties. Photovoltaic devices were fabricated in a typical sandwich structure of glass−ITO−PEDOT/PSS−polymer/PCBM−Al, where ITO and Al were

Table 1. Yield, Molecular Weight, PDI, and Decomposition Temperature of Nine Polymers

polymer	yield	M_n (kg/mol)[a]	M_w (kg/mol)[a]	PDI[a]	T_d[b] (°C)
PF-DTBT	54%	11.3	15.8	1.4	361
TP1	52%	4.2	5.7	1.4	300
TP2	57%	5.8	11.7	2.0	340
PC-DTBT	42%	16.5	24.8	1.5	371
TP3	32%	6.6	10.6	1.6	382
TP4	36%	7.8	14.0	1.8	317
PIC-DTBT	79%	17.5	33.9	1.9	344
TP5	73%	12.3	20.9	1.7	381
TP6	75%	14.4	26.4	1.8	387

[a] Determined by GPC with polystyrene as standard and $CHCl_3$ as eluent. [b] Onset decomposition temperature with 1% weight loss determined by TGA in air.

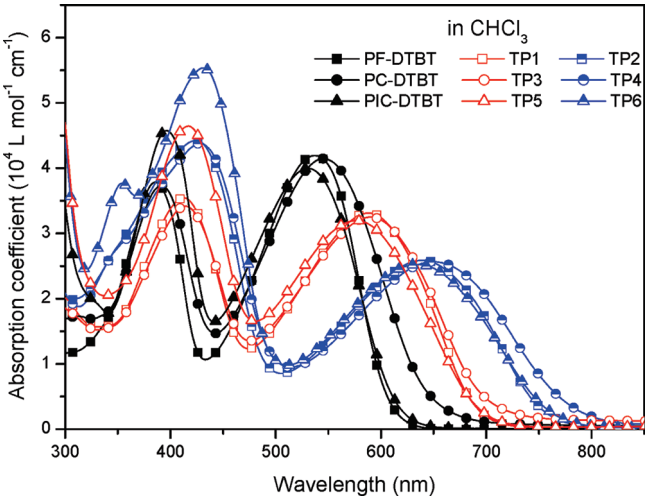

Figure 1. UV−vis absorption spectra of copolymers in $CHCl_3$ solution.

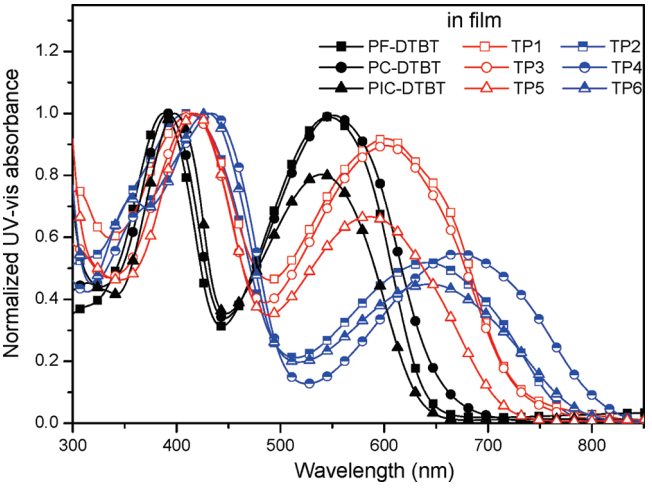

Figure 2. UV−vis absorption spectra of polymer films on a quartz plate.

used as anode and cathode, respectively, in diode-mode operation. The detailed layout and dimensions are shown in Scheme 4. The area of overlap between Al and ITO was approximately 3 × 5 mm^2. To avoid the so-called "edge effect" and evaluate the PCEs of the photovoltaic devices accurately,[18] we defined the effective area of the PSCs using a metal photomask (2 × 3 mm^2) during irradiation of simulated solar light.

Figure 4 shows the $I-V$ curves of the devices based on each of the nine polymers under illumination of AM 1.5 simulated solar light (100 mW/cm^2). The corresponding open-circuit voltage (V_{OC}), short-circuit current (I_{SC}), fill factor (FF), and PCE of the devices are summarized in Table 3.

The results indicate that the V_{OC} values of 0.80 to 1.02 V for the photovoltaic devices based on the three DTBT-based polymers were high, whereas those for polymers based on TP1-6 had lower V_{OC} values of 0.56 to 0.70 V. This difference in V_{OC} could result from the upward shift of the HOMO energy levels of DTTP-based polymers compared with DTBT-based polymers because the V_{OC} is related to the energy difference between the LUMO of the acceptor (PCBM) and the HOMO of the donor (the conjugated polymer).[19] In addition, all devices based on the six DTTP-based polymers exhibited lower PCEs than the DTBT-based polymers, which could be understood from two aspects: V_{OC}, which decreased because of an increase in the HOMO energy level of the DTTP-based polymers, and I_{SC}, which decreased probably because of the poor charge separation or transport of the DTTP-based polymers.

To compare the contribution of polymer absorption to I_{SC}, we measured the external quantum efficiency (EQE) of the devices based on three fluorene-containing polymers (PF-DTBT, TP1, and TP2) under the illumination of monochromatic light (Figure 5). The shape of the EQE curves of the devices was similar to that of the absorption spectra, indicating that all wavelengths absorbed by the polymers contributed to photovoltaic conversion. The maximum peak in the EQE curve was red-shifted from 530 (PF-DTBT) to 600 (TP1) and 640 nm (TP2), but the value of EQE decreased from 34% for PF-DTBT to 21% for TP1 and 16% for TP2. With increasing thickness of the active layer, the absorption could be improved, but the EQE value and I_{SC} decreased, possibly because the distance for the charge transport was too great. Further investigation on the charge transport properties in both the pristine polymer film and blend film are in progress.

For bulk-heterojunction polymer solar cells, it has been proposed that the surface morphology of the active layer strongly affects photovoltaic properties.[16j,20] The morphology of the blend films was observed by atomic force microscopy (AFM), as shown in Figure 6. All films, except TP5, exhibited low roughness and no significant aggregation, suggesting that those polymers were highly compatible with PCBM molecules in the films cast from the chlorobenzene solutions. The rough surface and coarse phase separation of the TP5/PCBM layer explain, at least in part, the lowest PCE of TP5, and suggest there is still high potential to improve the photovoltaic performance by developing suitable methods for controlling the morphology of TP5/PCBM.

The PCEs of the photovoltaic devices based on PF-DTBT/PCBM and PC-DTBT/PCBM were 2.67 and 3.05%, respectively, which were lower than the PCE values of similar materials in the literature.[8,9] Therefore, the preliminary photovoltaic performance still has high potential to be improved by intensive device optimization, such as changing the acceptor or cathode metal, controlling film morphology by slow growth and/or using mixed solvents. Further attempts to optimize the photovoltaic properties are in progress.

Conclusions

Six thieno[3,4-*b*]pyrazine-based donor−acceptor (D−A) copolymers (TP1-6) and three BT-based D−A copolymers (PF-DTBT, PC-DTBT, and PIC-DTBT) were synthesized by Suzuki cross-coupling reaction. The absorption peaks and absorption coefficients of the nine polymers were mainly dependent on the

Table 2. Optical and Electrochemical Properties, And Derived Energy Level of Nine Polymers

	UV−vis absorption spectrum				cyclic voltammetry		
	solution		film		*p*-doping	*n*-doping	
polymer	λ_{max} (nm)	absorption coefficient (L mol^{-1} cm^{-1})	λ_{max} (nm)	E_g^{opt} (eV)	E_{on}^{ox}/HOMO (V)/(eV)	E_{on}^{red}/LUMO (V)/(eV)	E_g^{EC} (eV)
PF-DTBT	386/537	4.19×10^4	387/547	1.85	0.76/−5.56	−1.33/- 3.47	2.09
TP1	412/588	3.31×10^4	414/600	1.61	0.46/−5.26	−1.35/−3.45	1.81
TP2	425/639	2.59×10^4	409/641	1.55	0.47/−5.27	−1.27/−3.53	1.74
PC-DTBT	391/545	4.15×10^4	392/551	1.72	0.68/−5.48	−1.34/−3.46	2.02
TP3	414/590	3.25×10^4	415/603	1.57	0.44/−5.24	−1.35/−3.45	1.79
TP4	428/651	2.57×10^4	434/674	1.46	0.43/−5.23	−1.25/−3.55	1.68
PIC-DTBT	397/531	4.00×10^4	398/540	1.91	0.65/−5.45	−1.25/−3.55	1.90
TP5	417/577	3.20×10^4	418/586	1.65	0.50/−5.30	−1.33/−3.47	1.83
TP6	431/635	2.52×10^4	430/644	1.51	0.52/−5.32	−1.21/−3.59	1.73

Scheme 4. Layout and Dimensions of Photovoltaic Device

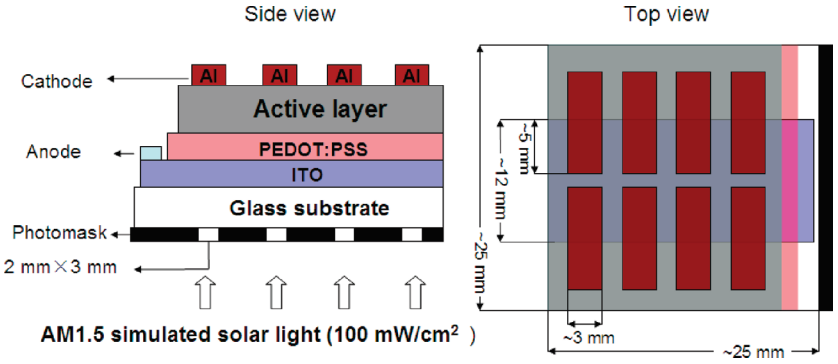

identity of the acceptors and the effects of the donor segments (fluorene, carbazole, and indolocarbazole) were small. The high-lying HOMO energy levels of six DTTP-based polymers were responsible for the lower V_{OC} of the PSCs. The results for the photovoltaic devices indicate that not only the position of absorption peaks but also the molecular energy levels should be considered carefully in the design of photovoltaic polymers.

Experimental Section

Synthesis. 9,9-Di(2-ethylhexyl)fluorene-2,7-diboronic acid bis(1,3-propanediol) ester solution (monomer **8**, 0.5 M in toluene, Aldrich) and other chemicals were purchased from Alfa, Aldrich, or Wako and used without further purification. The following compounds were synthesized according to the procedure in the literature: 4,7-di(2-bromothien-5-yl)-2,1,3-benzothiadiazole (monomer **1**),[17] 5,5″-dibromo-3′,4′-dinitro-2,2′:5′2″-terthiophene (**6**),[21] 2,7-bis-(4,4,5,5-tetramethyl-1,3,2-dioxaborolan-2-yl)-*N*-(1-decylundecyl)carbazole (monomer **9**),[22] and 3,9-bis(4,4,5,5-tetramethyl-1,3,2-dioxaborolan-2-yl)-5,11-di(1-decylundecyl)indolo[3,2-b]carbazole (monomer **10**).[15]

Synthesis of 2,3-Dimethyl-5,7-di(2-bromothien-5-yl)-thieno-[3,4-*b*]pyrazine (5a). 5,5″-Dibromo-3′,4′-dinitro-2,2′:5′2″-terthiophene (1.488 g, 3.0 mmol), iron powder (2.18 g, 39 mmol), and acetic acid (60 mL) were mixed and heated at 60 °C for 30 min. The mixture was cooled and filtered in a 100 mL flask. Then, 2,3-butanedione (0.77 g, 9.0 mmol) was added to the flask. The mixture was heated at 60 °C for 5 h under a N_2 atmosphere. After cooling, water was added, and the solid was collected by filtration and washed with CH_3OH. Finally, the crude compound was purified by column chromatography (silica gel; eluent: chloroform/hexane 50/50 (v/v)) and isolated as a deep red solid. Yield: 1.1 g (72%). ^{1}H NMR ($CDCl_3$, 400 MHz, δ): 7.22 (d, 2H), 7.02 (d, 2H), 2.64 (s, 6H). MALDI-TOF MS (m/z): calcd for $C_{16}H_{10}Br_2N_2S_3$, 483.84; found, 483.51.

Synthesis of 2,3-Diphenyl-5,7-di(2-bromothien-5-yl)-thieno-[3,4-*b*]pyrazine (5b). A procedure similar to the synthesis of **3a** was used starting from 5,5″-dibromo-3′,4′-dinitro-2,2′:5′2″-terthiophene (0.992 g, 2.0 mmol) and benzil (0.84 g, 4 mmol). The target compound was purified by column chromatography (silica gel; eluent: 50:50 chloroform/hexane v/v) and isolated as a black-blue solid. Yield: 0.82 g (67%). ^{1}H NMR ($CDCl_3$, 400 MHz, δ): 7.60−7.55 (m, 4H), 7.43−7.31 (m, 8H), 7.05 (m, 2H). MALDI-TOF MS (m/z): calcd for $C_{26}H_{14}Br_2N_2S_3$, 607.89; found, 607.42.

Synthesis of the Polymers by Suzuki Cross-Coupling Reaction. Monomers **8**, **9**, or **10** (0.4 mmol), monomers **1**, **5a**, or **5b** (0.38 mmol), and toluene (20 mL) were added to a 50 mL double-necked round-bottomed flask. The reaction container was purged with N_2 for 30 min to remove O_2. $Pd(PPh_3)_4$ (2%, 10 mg) was added and heated to 110 °C for 10 min. Tetraethylammonium hydroxide (1.8 mL, 20% by weight in H_2O) was introduced, and the mixture was heated under reflux overnight. Phenylboric acid (100 mg in 1 mL of THF) was added. After 2 h, bromobenzene (1 mL) was introduced. The mixture was allowed to reflux for 2 h and cooled to room temperature. Then, the polymer was precipitated by slow pouring of the mixture into MeOH, filtered, and Soxhlet extracted with ether and $CHCl_3$. The $CHCl_3$ solution was passed through a column packed with alumina, Celite, and silica gel. The column was eluted with $CHCl_3$. The combined polymer solution was concentrated to 30 mL and was poured in methanol (300 mL). The precipitate was collected and dried under vacuum overnight. The yield, ^{1}H NMR data ($CDCl_3$, 400 MHz), and molecular weight are as follows. **PC-DTBT**: Yield: 54%. ^{1}H NMR (δ): 8.19 (br, 2H), 7.95 (br, 2H), 7.74 (br, 6H), 7.49 (br, 2H), 2.14 (br, 4H), 1.0−0.5 (br, 30H). M_n = 11.3K; PDI = 1.4. **TP1**: Yield: 52%. ^{1}H NMR (δ): 7.8−7.4 (m, 10H), 2.74 (br, 6H), 2.11 (br, 4H), 1.0−0.5 (m, 30H). M_n = 4.2K; PDI = 1.4. **TP2**: Yield: 57%. ^{1}H NMR (δ): 7.8−7.3 (m, 20H), 2.11 (br, 4H), 1.0−0.5 (m, 30H). M_n = 5.8K; PDI = 2.0. **PC-DTBT**: Yield: 42%. ^{1}H NMR (δ): 8.1−7.4 (m, 12H), 4.70 (br, 1H), 2.40 (br, 2H), 2.02 (br, 2H), 1.4−0.7 (m, 38H). M_n = 16.5K; PDI = 1.5. **TP3**: Yield: 32%. ^{1}H NMR (δ): 8.1−7.3 (m, 10H), 4.68 (br, 1H), 2.74 (br, 6H), 2.41 (br, 2H), 2.03 (br, 2H), 1.4−0.7 (m, 38H). M_n = 6.6K; PDI = 1.6. **TP4**: Yield: 36%. ^{1}H NMR (δ): 8.1−7.3 (m, 20H), 4.70 (br, 1H), 2.41 (br,

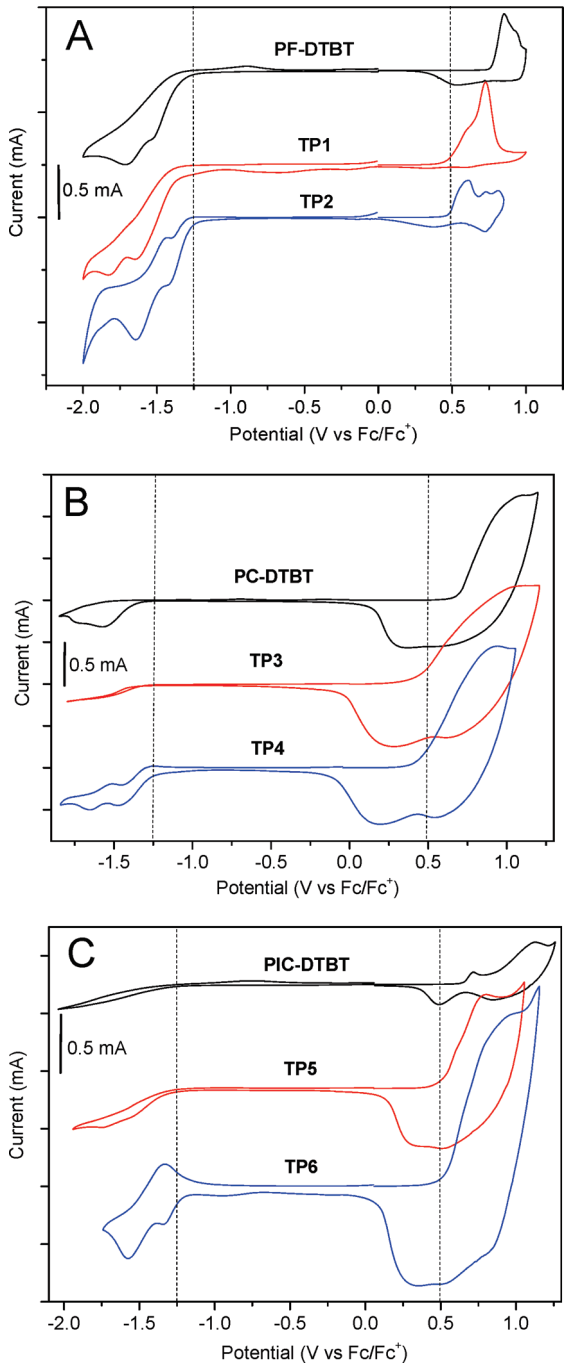

Figure 3. Cyclic voltammograms of nine polymers films on a platinum plate in acetonitrile solution of 0.1 mol/L $[Bu_4N]PF_6$ (Bu = butyl) at a scan rate of 50 mV/s. To highlight differences between polymers, dashed lines are drawn as a guide for the eyes.

2H), 2.02 (br, 2H), 1.4−0.7 (m, 38H). M_n = 7.8K; PDI = 1.8. **PIC-DTBT**: Yield: 79%. ^{1}H NMR (δ): 8.4−7.3 (m, 14H), 4.74 (br, 2H), 2.50 (br, 4H), 2.06 (br, 4H), 1.4−1.0 (br, 64H), 0.85 (m, 12H). M_n = 17.5K; PDI = 1.9. **TP5**: Yield: 73%. ^{1}H NMR (δ): 8.4−7.2 (m, 12H), 4.75 (br, 2H), 2.75 (br, 6H), 2.50 (br, 4H), 2.06 (br, 4H), 1.4−0.8 (m, 76H). M_n = 12.3K; PDI = 1.7. **TP6**: Yield: 75%. ^{1}H NMR (δ): 8.4−7.3 (m, 14H), 4.71 (br, 2H), 2.48 (br, 4H), 2.07 (br, 4H), 1.4−0.7 (m, 76H). M_n = 14.4K; PDI = 1.8.

Characterization. ^{1}H NMR (400 MHz) spectra were measured using a JEOL Alpha FT-NMR spectrometer equipped with an Oxford superconducting magnet system. Absorption spectra were measured using a Shimadzu MPC-3100 spectrophotometer. Cyclic voltammograms (CVs) were recorded on an

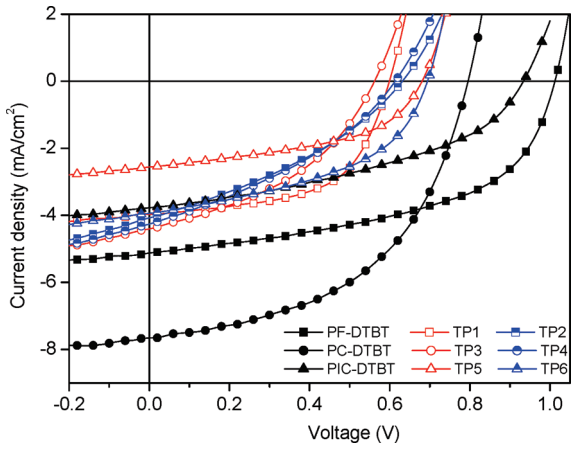

Figure 4. $I-V$ curves of nine polymer solar cells based various polymers under illumination of AM 1.5 at 100 mW/cm^2.

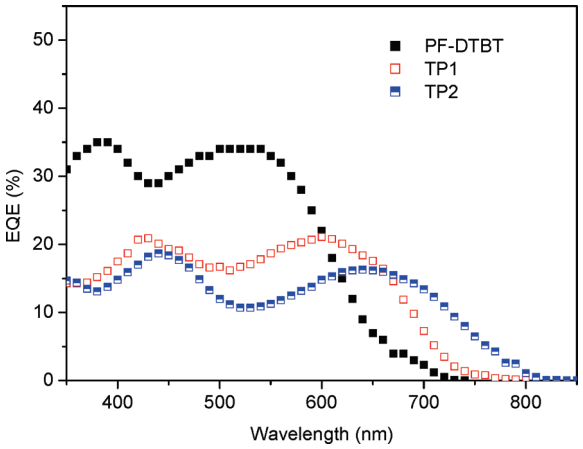

Figure 5. EQE of PSCs based on three fluorene-based polymers.

Table 3. Device Characteristics of PSCs Based on Nine Copolymers

active layer	V_{OC} (V)	I_{SC} (mA/cm^2)	FF	PCE (%)
PF-DTBT/PCBM	1.02	5.12	0.51	2.67
TP1/PCBM	0.60	3.97	0.57	1.37
TP2/PCBM	0.64	4.07	0.34	0.89
PC-DTBT/PCBM	0.80	7.66	0.50	3.05
TP3/PCBM	0.56	4.41	0.41	1.02
TP4/PCBM	0.62	3.94	0.37	0.90
PIC-DTBT/PCBM	0.94	3.77	0.41	1.47
TP5/PCBM	0.68	2.55	0.49	0.84
TP6/PCBM	0.70	3.94	0.46	1.27

HSV-100 (Hokuto Denkou) potentiostat. A Pt plate coated with a thin polymer film was used as the working electrode. A Pt wire and an Ag/Ag$^+$ (0.01 M of $AgNO_3$ in acetonitrile) electrode were used as the counter and reference electrodes (calibrated against Fc/Fc+), respectively. AFM measurement was carried out using a Digital Instrumental Nanoscope 31 operated in tapping mode.

Fabrication and Characterization of Polymer Solar Cells. PSCs were constructed in the traditional sandwich structure through several steps. ITO-coated glass substrates were cleaned by ultrasonication sequentially in detergent, water, acetone, and 2-propanol. After drying the substrate, PEDOT/PSS (Baytron P), was spin-coated (4000 rpm for 30 s) on ITO. The film was dried at 150 °C under a N_2 atmosphere for 5 min. After the substrate was cooled, a chlorobenzene solution of the polymer and PCBM mixture was spin-coated. After the chlorobenzene was dried, the substrate was transferred into an evaporation

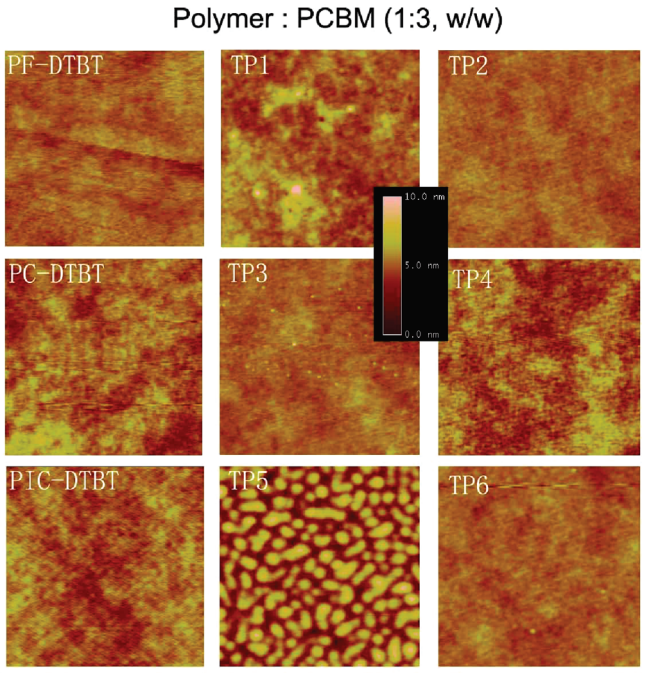

Figure 6. AFM height images of polymer/PCBM (1:3, w/w) composite film, spin-coated from chlorobenzene solution; image window is 2 × 2 μm^2 except for PIC-DTBT (1 × 1 μm^2).

chamber (ALS technology, H-2807 vacuum evaporation system with E-100 load lock). An Al electrode (~60 nm) was evaporated onto the substrate under high vacuum (10^{-4} to 10^{-5} Pa). Post-device annealing was carried out at 110 °C for 5 min inside a nitrogen-filled glovebox. The current−voltage characteristics of the photovoltaic cells were measured using a Keithley 2400 I−V measurement system. The measurements were conducted under the irradiation of AM 1.5 simulated solar light (100 mW cm^{-2}, Peccell Technologies, PCE-L11). Light intensity was adjusted by using a standard silicon solar cell with an optical filter (Bunkou Keiki, BS520). The EQE of the devices was measured on a Hypermonolight System (Bunkou Keiki, SM-250F).

References and Notes

(1) (a) Yu, G.; Hummelen, J.; Wudl, F.; Heeger, A. J. *Science* **1995**, *270*, 1789. (b) Dennler, G.; Scharber, M. C.; Brabec, C. J. *Adv. Mater.* **2009**, *21*, 1323. (c) Krebs, F. C. *Sol. Energy. Mater. Sol. Cells* **2009**, *93*, 394. (d) Krebs, F. C.; Gevorgyan, S. A.; Alstrup, J. *J. Mater. Chem.* **2009**, *19*, 5442. (e) Helgesen, M.; Sondergaard, R.; Krebs, F. C. *J. Mater. Chem.* **2010**, *20*, 36.

(2) (a) Li, G.; Shrotriya, V.; Huang, J. S.; Yao, Y.; Moriarty, T.; Emery, K.; Yang, Y. *Nat. Mater.* **2005**, *4*, 864. (b) Ma, W. L.; Yang, C. Y.; Gong, X.; Lee, K.; Heeger, A. J. *Adv. Funct. Mater.* **2005**, *15*, 1617.

(3) (a) Winder, C.; Sariciftci, N. S. *J. Mater. Chem.* **2004**, *14*, 1077. (b) Bundgaard, E.; Krebs, F. C. *Sol. Energy. Mater. Sol. Cells* **2007**, *91*, 954. (c) Li, Y. F.; Zou, Y. P. *Adv. Mater.* **2008**, *20*, 2952.

(4) (a) Roncali, J. *Chem. Rev.* **1997**, *97*, 173. (b) Ajayaghosh, A. *Chem. Soc. Rev.* **2003**, *32*, 181.

(5) (a) Peet, J.; Kim, J. Y.; Coates, N. E.; Ma, W. L.; Moses, D.; Heeger, A. J.; Bazan, G. C. *Nat. Mater.* **2007**, *6*, 497. (b) Hou, J. H.; Chen, H. Y.; Zhang, S. Q.; Li, G.; Yang, Y. *J. Am. Chem. Soc.* **2008**, *130*, 16144. (c) Liang, Y. Y.; Feng, D. Q.; Wu, Y.; Tsai, S.-T.; Li, G.; Ray, C.; Yu, L. P. *J. Am. Chem. Soc.* **2009**, *131*, 7792. (d) Park, S. H.; Roy, A.; Beaupré, S.; Cho, S.; Coates, N.; Moon, J. S.; Moses, D.; Leclerc, M.; Lee, K.; Heeger, A. J. *Nat. Photonics* **2009**, *3*, 297. (e) Chen, H.-Y.; Hou, J. H.; Zhang, S. Q.; Liang, Y. Y.; Yang, G. W.; Yang, Y.; Yu, L. P.; Wu, Y.; Li, G. *Nat. Photonics* **2009**, *3*, 649.

(6) (a) Dhanabalan, A.; van Duren, J. K. J.; van Hal, P. A.; van Dongen, J. L. J.; Janssen, R. A. J. *Adv. Funct. Mater.* **2001**, *11*, 255–262. (b) Brabec, C. J.; Winder, C.; Sariciftci, N. S.; Hummelen, J. C.; Dhanabalan, A.; van Hal, P. A.; Janssen, R. A. J. *Adv. Funct. Mater.* **2002**, *12*, 709.

(7) Liu, C. L.; Tsai, J. H.; Lee, W. Y.; Chen, W. C.; Jenekhe, S. A. *Macromolecules* **2008**, *41*, 6952.

(8) (a) Svensson, M.; Zhang, F. L.; Veenstra, S. C.; Verhees, W. J. H.; Hummelen, J. C.; Kroon, J. M.; Inganäs, O.; Andersson, M. R. *Adv. Mater.* **2003**, *15*, 988. (b) Chen, M. -H.; Hou, J. H.; Hong, Z. R.; Yang, G. W.; Sista, S.; Chen, L.-M.; Yang, Y. *Adv. Mater.* **2009**, *21*, 4238.

(9) (a) Blouin, N.; Michaud, A.; Leclerc, M. *Adv. Mater.* **2007**, *19*, 2295. (b) Chu, T.-Y; Alem, S.; Verly, P. G.; Wakim, S.; Lu, J. P.; Tao, Y.; Beaupré, S.; Leclerc, M.; Bélanger, F.; Désilets, D.; Rodman, S.; Waller, D.; Gaudiana, R. *Appl. Phys. Lett.* **2009**, *95*, 063304.

(10) (a) Boudreault, P. T.; Michaud, A.; Leclerc, M. *Macromol. Rapid Commun.* **2007**, *28*, 2176. (b) Wang, E. G.; Wang, L.; Lan, L. F.; Luo, C.; Zhuang, W. L.; Peng, J. B.; Cao, Y. *Appl. Phys. Lett.* **2008**, *92*, 033307.

(11) Song, S.; Jin, Y.; Kim, S. H.; Moon, J.; Kim, K.; Kim, J. Y.; Park, S. H.; Lee, K.; Suh, H. *Macromolecules* **2008**, *41*, 7296.

(12) Moulé, A. J.; Tsami, A.; Bünnagel, T. W.; Forster, M.; Kronenberg, N. M.; Scharber, M.; Koppe, M.; Morana, M.; Brabec, C. J.; Meerholz, K.; Scherf, U. *Chem. Mater.* **2008**, *20*, 4045.

(13) (a) Liao, L.; Dai, L. M.; Smith, A.; Durstock, M.; Lu, J. P.; Ding, J. F.; Tao, Y. *Macromolecules* **2007**, *40*, 9406. (b) Huo, L. J.; Chen, H.-Y.; Hou, J. H.; Chen, T. L.; Yang, Y. *Chem. Commun.* **2009**, 5570.

(14) Zhou, E. J.; Nakamura, M.; Nishizawa, T.; Zhang, Y.; Wei, Q. S.; Tajima, K.; Yang, C. H.; Hashimoto, K. *Macromolecules* **2008**, *41*, 8302.

(15) Zhou, E. J.; Yamakawa, S.; Tajima, K.; Yang, C. H.; Hashimoto, K. *J. Mater. Chem.* **2009**, *19*, 7730.

(16) (a) Zhang, F. L.; Perzon, E.; Wang, X. J.; Mammo, W.; Andersson, M. R.; Inganäs, O. *Adv. Funct. Mater.* **2005**, *15*, 745. (b) Xia, Y. J.; Luo, J.; Deng, X. Y.; Li, X. Z.; Li, D. Y.; Zhu, X. H.; Yang, W.; Cao, Y. *Macromol. Chem. Phys.* **2006**, *207*, 511. (c) Zhang, F. L.; Mammo, W.; Andersson, L. M.; Admassie, S.; Andersson, M. R.; Inganäs, O. *Adv. Mater.* **2006**, *18*, 2169. (d) Ashraf, R. S.; Shahid, M.; Klemm, E.; Al-Ibrahim, M.; Sensfuss, S. *Macromol. Rapid Commun.* **2006**, *27*, 1454. (e) Wienk, M. M.; Turbiez, M. G. R.; Struijk, M. P.; Fonrodona, M.; Janssen, R. A. J. *Appl. Phys. Lett.* **2006**, *88*, 153511. (f) Zhu, Y.; Champion, R. D.; Jenekhe, S. A. *Macromolecules* **2006**, *39*, 8712. (g) Petersen, M. H.; Hagemann, O.; Nielsen, K. T.; Jorgensen, M.; Krebs, F. C. *Sol. Energy Mater. Sol. Cells* **2007**, *91*, 996. (h) Petersen, M. H.; Gevorgyan, S. A.; Krebs, F. C. *Macromolecules* **2008**, *41*, 8986. (i) Becerril, H. A.; Miyaki, N.; Tang, M. L.; Mondal, R.; Sun, Y.-S.; Mayer, A. C.; Parmer, J. E.; McGehee, M. D.; Bao, Z. N. *J. Mater. Chem.* **2009**, *19*, 591. (j) Bull, T. A.; Pingree, L. S. C.; Jenekhe, S. A.; Ginger, D. S.; Luscombe, C. K. *ACS Nano* **2009**, *3*, 627.

(17) Hou, Q.; Xu, Y. S.; Yang, W.; Yuan, M.; Peng, J. B.; Cao, Y. *J. Mater. Chem.* **2002**, *12*, 2887.

(18) Scharber, M. C.; Müehlbacher, D.; Koppe, M.; Denk, P.; Waldauf, C.; Heeger, A. J.; Brabec, C. *J. Adv. Mater.* **2006**, *18*, 789.

(19) (a) Mihailetchi, V. D.; M. Blorn, P. W.; Hummelen, J. C.; Rispens, M. T. *J. Appl. Phys.* **2003**, *94*, 6849. (b) Dyakonov, V. *Appl. Phys. A: Mater. Sci. Process.* **2004**, *79*, 21.

(20) Chen, L.-M.; Hong, Z. R.; Li, G.; Yang, Y. *Adv. Mater.* **2009**, *21*, 1434.

(21) Mammo, W.; Admassie, S.; Gadisa, A.; Zhang, F. L.; Inganäs, O.; Andersson, M. R. *Sol. Energy Mater. Sol. Cells* **2007**, *91*, 1010.

(22) Zhou, E. J.; Yamakawa, S.; Tajima, K.; Yang, C. H.; Hashimoto, K. *Chem. Mater.* **2009**, *21*, 4055.